

# Electron Deficiency in Tetrahedral Transition-Metal Clusters: Electronic Structure and Magnetic Properties of $[\text{Ru}_4(\eta^6\text{-C}_6\text{H}_6)_4(\mu_3\text{-H})_4]^{2+}$

Régis Gautier,<sup>†</sup> Frédéric Chérioux,<sup>‡</sup> Georg Süss-Fink,<sup>\*,†</sup> and Jean-Yves Saillard<sup>\*,§</sup>

Département de Physicochimie, UPRES-1795, Ecole Nationale Supérieure de Chimie de Rennes, Institut de Chimie de Rennes, F-35700 Rennes, France, Institut de Chimie, Université de Neuchâtel, Case postale 2, CH-2007 Neuchâtel, Switzerland, and Institut de Chimie de Rennes, Université de Rennes 1, F-35042 Rennes Cedex, France

Received February 6, 2003

Analysis of the electronic structure of the electron-deficient cluster cation  $[\text{Ru}_4(\eta^6\text{-C}_6\text{H}_6)_4\text{H}_4]^{2+}$  ( $1^{2+}$ ) by density functional theory calculations shows a very small energy gap (0.06 eV) between the diamagnetic singlet state and the paramagnetic triplet state, as a consequence of the absence of a significant Jahn–Teller distortion in the molecular structure of  $1^{2+}$ . Magnetic measurements of  $[\text{1}]\text{Cl}_2$ ,  $[\text{1}]\text{[BF}_4\text{]}_2$ , and  $[\text{1}]\text{[PF}_6\text{]}_2$  show  $1^{2+}$  to be diamagnetic in the fundamental state, with some weak temperature-independent paramagnetism, depending upon the nature of the counterion.

## Introduction

In the same manner as tetrahedrane does, most of the known organometallic tetrahedral clusters containing transition-metal atoms exhibit a localized 2-electron/2-center bonding mode in which the four atoms constituting the tetrahedral skeleton satisfy the effective atomic number (EAN) rule, i.e., the octet and 18-electron rule for the main group and transition-metal elements, respectively.<sup>1</sup> This is the case for the tetranuclear clusters  $\text{M}_4(\text{CO})_{12}$  ( $\text{M} = \text{Co}$ ,  $\text{Rh}$ ,  $\text{Ir}$ ),<sup>2</sup> for which the total of 60 metal valence electrons (MVEs) is consistent with the existence of four 18-electron metal centers and six 2-electron metal–metal bonds ( $4 \times 18 - 6 \times 2 = 60$ ).

The tetranuclear benzene cluster dications  $[\text{Ru}_4(\eta^6\text{-C}_6\text{H}_6)_4\text{H}_4]^{2+}$  ( $1^{2+}$ ) and  $[\text{Ru}_4(\eta^6\text{-C}_6\text{H}_6)_4\text{H}_6]^{2+}$  ( $2^{2+}$ ) not only

deviate from these simple electron count/structure relationships but also have a rather complex and confusing history: We obtained  $2^{2+}$  in 1993 from the reaction of a (benzene)-ruthenium dichloride dimer with molecular hydrogen in aqueous solution under high-pressure conditions. In the single-crystal X-ray structure analysis of the chloride salt of  $2^{2+}$  (violet crystals), we found only four of the six hydrides, which prompted us to publish  $2^{2+}$  erroneously as  $[\text{Ru}_4(\eta^6\text{-C}_6\text{H}_6)_4\text{H}_4]^{2+}$ .<sup>3</sup> As we obtained this tetrahydrido cluster dication  $1^{2+}$  in 1994, the chloride salt (black-brown crystals) being distinctly different of that of  $2^{2+}$ , we established the formula of  $[\text{Ru}_4(\eta^6\text{-C}_6\text{H}_6)_4\text{H}_6]^{2+}$  for  $2^{2+}$  on the basis of the integral ratio of the proton NMR signal of the hydrides with respect to that of the benzene protons (6:24). Finally, we were able to locate the six hydrides in the crystal structure analysis of the *p*-cymene analogue  $[\text{Ru}_4(\eta^6\text{-}p\text{-MeC}_6\text{H}_4\text{-Pr}^i)_4\text{H}_6]^{2+}$  ( $3^{2+}$ ; perchlorate salt).<sup>4</sup> The tetrahydrido cluster **1** turned out to be the parent complex of the *p*-cymene analogue  $[\text{Ru}_4(\eta^6\text{-}p\text{-MeC}_6\text{H}_4\text{Pr}^i)_4\text{H}_6]^{2+}$  ( $4^{2+}$ ) already known.<sup>5</sup>

The deformation of the hexahydrido clusters  $2^{2+}$  and  $3^{2+}$  (60-MVE species) from tetrahedral symmetry in the crystal was quite unexpected: The  $\text{Ru}_4$  tetrahedron is distinctly distorted, and the six hydride ligands were not found as  $\mu_2$

\* Authors to whom correspondence should be addressed. E-mail: saillard@univ-rennes1.fr (J.-Y.S.); georg.suess-fink@unife.ch (G.S.-F.).

<sup>†</sup> Ecole Nationale Supérieure de Chimie de Rennes.

<sup>‡</sup> Université de Neuchâtel.

<sup>§</sup> Université de Rennes 1.

- (1) For a general overview on bonding in transition-metal clusters, see for example: (a) *Transition Metal Clusters*; Johnson, B. F. G., Ed.; John Wiley and Sons: Chichester, U.K., 1980. (b) *Metal Clusters*; Moskovits, M., Ed.; John Wiley and Sons: New York, 1986. (c) Mingos, D. M. P.; Wales, D. J. *Introduction to Cluster Chemistry*; Prentice Hall International Editions: Englewood Cliffs, NJ, 1990. (d) *The Chemistry of Metal Cluster Complexes*; Shriver, D. F., Kaesz, H. D., Adams, R. D., Eds.; VCH: New York, 1990. (e) *Clusters and Colloids. From Theory to Application*; Schmid, G., Ed.; VCH: Weinheim, Germany, 1994.
- (2) (a) Carre, F. H.; Cotton, F. A.; Frez, B. A. *Inorg. Chem.* **1976**, *15*, 380. (b) Wei, C. H. *Inorg. Chem.* **1969**, *11*, 2384. (c) Churchill, M. R.; Hutchinson, J. P. *Inorg. Chem.* **1978**, *17*, 3528.

(3) Bodensieck, U.; Meister, A.; Meister, G.; Rheinwald, G.; Stoeckli-Evans, H.; Süss-Fink, G. *Chimia* **1993**, *47*, 189.

(4) Meister, G.; Rheinwald, G.; Stoeckli-Evans, H.; Süss-Fink, G. *J. Chem. Soc., Dalton Trans.* **1994**, 3215.

(5) Cabeza, J. A.; Nutton, A.; Mann, B. E.; Brevard, C.; Maitlis, P. M. *Inorg. Chim. Acta* **1986**, *115*, L47.

bridges over the six Ru–Ru bonds, as expected from the single hydride resonance of  $\delta = -15.03(\text{s})$  and  $-15.83(\text{s})$  observed for  $2^{2+}$  and  $3^{2+}$ , respectively, in a  $\text{D}_2\text{O}$  solution.<sup>4,6</sup> A reexamination of the single-crystal X-ray structure analysis of  $2^{2+}$  (chloride salt) suggested the so-called hexahydrido complex to contain an intact  $\text{H}_2$  ligand and to represent in reality a tetrahydrido–dihydrogen cluster  $[\text{Ru}_4(\eta^6\text{-C}_6\text{H}_6)_4\text{H}_4(\eta^2\text{-}\mu_3\text{-H}_2)]^{2+}$ ; this interpretation was confirmed by NMR  $T_1$  measurements at  $-120^\circ\text{C}$  and by density functional theory (DFT) calculations.<sup>7</sup>

While the distorted tetrahedral structure of the 60-MVE hexahydrido cluster  $2^{2+}$  found its explanation in the presence of an intact dihydrogen ligand, the nondistorted tetrahedral structure of the 58-MVE tetrahydrido cluster  $1^{2+}$  remained mysterious because a Jahn–Teller distortion or a paramagnetic behavior is, in principle, expected for a tetrahedral cluster with an electron count of 58 MVE, although there is no full guarantee that a partially filled degenerate set of orbitals would lead to a triplet state.<sup>8</sup> To find out the reason for this remarkable behavior, we carried out a combined theoretical and magnetochemical study of the electron-deficient cluster dication  $1^{2+}$ .

## Experimental Section

**Computational Details.** DFT calculations were carried out using the Amsterdam Density Functional (ADF) program<sup>9</sup> developed by Baerends and co-workers.<sup>10</sup> Becke exchange<sup>11</sup> and Perdew correlation<sup>12</sup> nonlocal gradient corrections were included in the local density approximation.<sup>13</sup> The geometry optimization was based on the method developed by Versluis and Ziegler.<sup>14</sup> The Slater-type basis was of triple- $\zeta$  quality. A single- $\zeta$  5p polarization function, as well as a single- $\zeta$  3d one in the C valence set and a single- $\zeta$  2p one in the H basis set, was included in the Ru valence set. A frozen-core approximation<sup>10a</sup> was used to treat the core electrons of Ru (1s–4p) and C (1s).

**Preparation of the Samples.** The cluster cation  $1^{2+}$  was synthesized according to the published procedure from  $[\text{Ru}(\eta^6\text{-C}_6\text{H}_6)\text{Cl}_2]_2$  and  $\text{H}_2$  in aqueous solution and isolated as the chloride salt.<sup>4</sup> The tetrafluoroborate and hexafluorophosphate salts were prepared by precipitation of  $[\mathbf{1}][\text{BF}_4]_2$  or  $[\mathbf{1}][\text{PF}_6]_2$  from the aqueous solution of  $[\mathbf{1}]\text{Cl}_2$  upon addition of an equimolar  $\text{NaBF}_4$  or  $\text{KPF}_6$  solution. The samples of  $[\mathbf{1}]\text{Cl}_2$ ,  $[\mathbf{1}][\text{BF}_4]_2$ , and  $[\mathbf{1}][\text{PF}_6]_2$  were isolated by filtration using glass ceramic filters and metal-free spatulas, washed with water, and dried in vacuo.

**Magnetic Measurements.** Temperature-dependent (2–298 K) magnetization data were recorded at the Max-Planck-Institut für Strahlenchemie, Mülheim an der Ruhr, Germany, using a SQUID magnetometer (MPMS-7, Quantum Design) in an external field of 1.0 T. The experimental susceptibility data were corrected for underlying diamagnetism by use of tabulated Pascal's constants.

## Results and Discussion

In the 60-MVE clusters  $2^{2+}$  and  $3^{2+}$ , the bridging hydrogen ligands provide to the  $[\text{Ru}_4(\text{arene})_4]^{2+}$  framework the six extra electrons necessary for 60 MVE, consistent with the EAN rule. This electron count is typical for a cluster with a significant highest occupied molecular orbital (HOMO)/lowest unoccupied molecular orbital (LUMO) gap, allowing the molecule to satisfy the closed-shell requirement. When this stability rule is reached, the six skeletal orbitals that are occupied correspond (assuming ideal  $T_d$  symmetry) to strongly bonding  $a_1$  and  $t_2$  levels and to a weakly bonding  $e$  level, which is generally the highest-occupied level of the cluster. The six antibonding skeletal molecular orbitals (MOs) are of  $t_1$  and  $t_2$  symmetry. They are high-lying and vacant.<sup>1c</sup> Their occupation would lead to bond breaking, generating more open geometries exhibiting the framework of a butterfly or a square.<sup>1</sup> On the other hand, the effect of electron deficiency on the tetrahedral cluster core is less straightforward. For example, the simple  $\text{B}_4\text{X}_4$  ( $\text{X} = \text{halide}$ ) 4-electron-deficient series is known to exhibit a perfect  $T_d$  geometry, with its skeleton MOs of  $e$  symmetry being fully unoccupied.<sup>1c</sup> In principle, the partial occupation of this  $e$  level is expected to generate Jahn–Teller instability, which should lead to a distortion away from the ideal tetrahedral geometry. To our knowledge, only two strongly related examples of 2-electron-deficient (i.e., 58-MVE) transition-metal homotetranuclear tetrahedral organometallic clusters have been structurally characterized to date, namely,  $1^{2+}$  (chloride salt)<sup>4</sup> and  $[\text{Rh}_4(\eta^5\text{-C}_5\text{Me}_5)_4(\mu_3\text{-H})_4]^{2+}$  ( $5^{2+}$ , tetrafluoroborate salt).<sup>15,16,17</sup> Both room temperature and low-temperature X-ray molecular structures of cluster  $5^{2+}$  exhibit some distortion toward approximate  $D_{2d}$  symmetry with four long (2.829 Å) and two short (2.610 Å) Rh–Rh distances. On the other hand, the room-temperature X-ray molecular structure of compound  $1^{2+}$  does not exhibit significant distortion away from the ideal  $T_d$  symmetry, with almost equal Ru–Ru bonds (ca. 2.73 Å) and each of the H atoms capping regularly one of the triangular faces of the tetrahedron, as exemplified by the major X-ray data of  $1^{2+}$ , which are given in Table 1.<sup>4</sup> Unfortunately, no low-temperature X-ray data on compounds of type **1** are available.

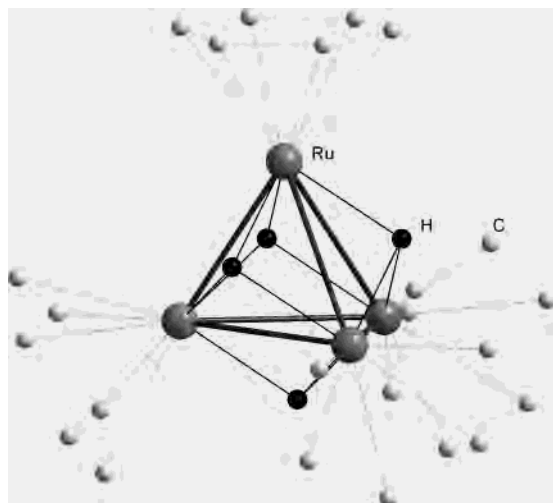
Given that the single-crystal X-ray structure analysis of  $1^{2+}$  (chloride salt) reveals a tetrahedral molecule close to  $T_d$  symmetry,<sup>4</sup> this dication is likely to possess a half-occupied

- (6) Plasseraud, L.; Süß-Fink, G. *J. Organomet. Chem.* **1997**, 539, 163.  
 (7) Süß-Fink, G.; Plasseraud, L.; Maisse-François, A.; Stoeckli-Evans, H.; Berke, H.; Fox, T.; Gautier, R.; Saillard, J.-Y. *J. Organomet. Chem.* **2000**, 609, 196.  
 (8) (a) Borden, W. T.; Iwamura, H.; Berson, J. A. *Acc. Chem. Res.* **1994**, 27, 109. (b) Shiota, Y.; Kondo, M.; Yoshizawa, K. *J. Chem. Phys.* **2001**, 115, 9243.  
 (9) *Amsterdam Density Functional (ADF) program*, release 2.3; Vrije Universiteit: Amsterdam, The Netherlands, 1997.  
 (10) (a) Baerends, E. J.; Ellis, D. E.; Ros, P. *Chem. Phys.* **1973**, 2, 41. (b) Baerends, E. J.; Ros, P. *Int. J. Quantum Chem.* **1978**, S12, 169. (c) Boerrigter, P. M.; te Velde, G.; Baerends, E. J. *Int. J. Quantum Chem.* **1988**, 33, 87. (d) te Velde, G.; Baerends, E. J. *J. Comput. Phys.* **1992**, 99, 84.  
 (11) Becke, A. D. *Phys. Rev. A* **1988**, A38, 3098.  
 (12) (a) Perdew, J. P. *Phys. Rev. B* **1986**, 33, 8822. (b) Perdew, J. P. *Phys. Rev. B* **1986**, 34, 7046.  
 (13) Vosko, S. H.; Wilk, L.; Nusair, M. *Can. J. Phys.* **1980**, 58, 1200.  
 (14) Versluis, L.; Ziegler, T. J. *J. Chem. Phys.* **1988**, 88, 322.

- (15) Espinet, P.; Bailey, P. M.; Piraino, P.; Maitlis, P. M. *Inorg. Chem.* **1979**, 18, 2706.  
 (16) Ricci, J. S.; Koetzle, T. F.; Goodfellow, B. J.; Espinet, P.; Maitlis, P. M. *Inorg. Chem.* **1984**, 23, 1828.  
 (17) Distorted tetrahedral 58-MVE heterotetranuclear organometallic clusters are known. See for example: Braunstein, P.; de Méric de Bellefond, C.; Bouaoud, S.-E.; Grandjean, D.; Halet, J.-F.; Saillard, J.-Y. *J. Am. Chem. Soc.* **1991**, 113, 5282.

**Table 1.** Experimental Distances of  $[\text{Ru}_4(\eta^6\text{-C}_6\text{H}_6)_4\text{H}_4]^{2+}$  ( $\mathbf{1}^{2+}$ ), Energy Differences, and Computed Distances of  $[\text{Ru}_4(\eta^6\text{-C}_6\text{H}_6)_4\text{H}_4]^{n+}$  ( $n = 0, 2$ )

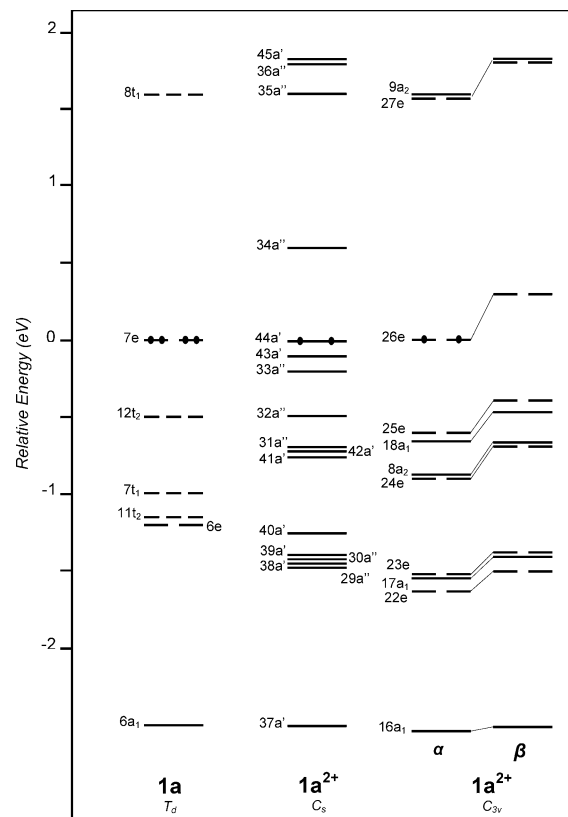
	experimental <sup>3</sup>	$[\text{Ru}_4(\eta^6\text{-C}_6\text{H}_6)_4\text{H}_4]^{2+}$ $C_s$ , singlet	$[\text{Ru}_4(\eta^6\text{-C}_6\text{H}_6)_4\text{H}_4]^{2+}$ $C_{3v}$ , triplet	$\text{Ru}_4(\eta^6\text{-C}_6\text{H}_6)_4\text{H}_4 T_d$
Ru–Ru (Å)	2.729 (×3) 2.730 (×3)	2.64 2.83 (×2) 2.83 (×2) 2.64	2.75 (×3) 2.75 (×3)	2.78 (×6)
Ru–H (Å)	2.02 (×6) 1.83 (×3) 2.20 (×3)	1.87 1.88 (×2) 1.91 (×2) 1.91 (×2) 1.86 (×2) 1.88 (×2) 1.88 (×2)	1.89 (×3) 1.88 (×6) 1.89 (×3)	1.87 (×12)
Ru–C(av) (Å)	2.18	2.31	2.32	2.30
$\Delta E$ (eV)		0	+0.06	

**Figure 1.** DFT-optimized structure of  $[\text{Ru}_4(\eta^6\text{-C}_6\text{H}_6)_4\text{H}_4]^{2+}$  ( $\mathbf{1}^{2+}$ ) (singlet state).

doubly degenerate e HOMO.<sup>18</sup> This raises the following questions: (i) Why does  $\mathbf{1}^{2+}$  not show a significant Jahn–Teller distortion away from  $T_d$ , despite this electronic degeneracy? (ii) Why does  $\mathbf{1}^{2+}$  show an unperturbed  $^1\text{H}$  NMR spectrum like a diamagnetic complex, although without significant Jahn–Teller distortion it should be paramagnetic?

DFT geometry optimizations on  $\mathbf{1}$  and on the singlet and triplet states of  $\mathbf{1}^{2+}$  have been carried out at the nonlocal level, assuming  $T_d$ ,  $C_s$ , and  $C_{3v}$  symmetries. The major results are given in Table 1. The molecular structure corresponding to the singlet state of  $\mathbf{1}^{2+}$  is shown in Figure 1. The MO diagrams of  $\mathbf{1}$  and  $\mathbf{1}^{2+}$  (singlet and triplet states) are sketched in Figure 2. Calculations on the 60-MVE cluster  $\mathbf{1}$  confirm the expectation of a weakly metal–metal bonding doubly degenerate HOMO (Figure 2). From the relative isolation in the energy scale of this HOMO from the other occupied MOs, there is strong evidence that the oxidation of  $\mathbf{1}$  is going to take place on this e level. This is confirmed by our calculations on  $\mathbf{1}^{2+}$  assuming  $T_d$  symmetry, which lead to a half-occupied e level. However, none of the singlet and triplet state geometries was found to be rigorously of  $T_d$  symmetry.

The optimization of the triplet state in the  $C_{3v}$  symmetry provides a structure that is slightly more stable than the  $T_d$  geometry (by 0.02 eV) and is very close to that obtained

**Figure 2.** DFT-MO diagrams for  $\text{Ru}_4(\eta^6\text{-C}_6\text{H}_6)_4\text{H}_4$  ( $\mathbf{1}$ ) (left) and  $[\text{Ru}_4(\eta^6\text{-C}_6\text{H}_6)_4\text{H}_4]^{2+}$  ( $\mathbf{1}^{2+}$ ) (middle, singlet; right, triplet). Only HOMOs are filled with electrons. Their energies are arbitrarily set to zero.

under  $T_d$  symmetry. If significant, this difference should arise from very small steric or electronic effects. As expected from the weak bonding character of their e HOMO, the Ru–Ru distances (2.75 Å) of  $\mathbf{1}^{2+}$  are slightly longer than those of  $\mathbf{1}$ . The Ru–Ru and Ru–C distances optimized in the triplet state of  $\mathbf{1}^{2+}$  are somewhat longer than the experimental ones (Table 1). This is likely to come from the nonlocal DFT approximation, which often tends to overestimate metal–metal and metal–ligand separations.<sup>19</sup>

As expected, a lowering of the symmetry to  $C_s$  tends to stabilize this singlet ground-state molecule. However, the stabilization is moderate (0.28 eV). Nevertheless, the HOMO/LUMO energy splitting is significant (0.60 eV). The geo-

(18) Hoffmann, R.; Schilling, B. E. R.; Bau, R.; Kaesz, H. D.; Mingos, D. M. P. *J. Am. Chem. Soc.* **1978**, *100*, 6088.

(19) Garland, M. T.; Halet, J.-F.; Saillard, J.-Y. *Inorg. Chem.* **2001**, *40*, 3342.

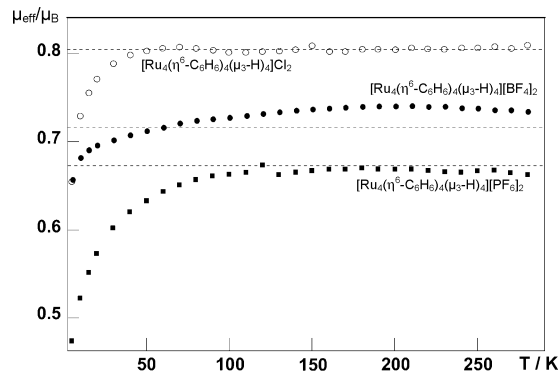
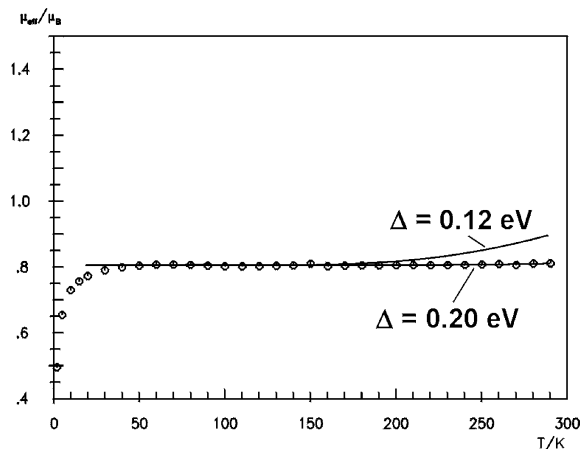
**Table 2.** Experimental Distances of  $[\text{Rh}_4(\eta^5\text{-C}_5\text{Me}_5)_4\text{H}_4]^{2+}$  ( $5^{2+}$ ), Energy Differences, and Computed Distances of  $[\text{Rh}_4(\eta^5\text{-C}_5\text{H}_5)_4\text{H}_4]^{n+}$  ( $6^{n+}$ ;  $n = 0, 2$ )

	$[\text{Rh}_4(\eta^5\text{-C}_5\text{Me}_5)_4\text{H}_4]^{2+}$ experimental <sup>5b</sup>	$[\text{Rh}_4(\eta^5\text{-C}_5\text{H}_5)_4\text{H}_4]^{2+}$ $C_s$ , singlet	$[\text{Rh}_4(\eta^5\text{-C}_5\text{H}_5)_4\text{H}_4]^{2+}$ $C_s$ , triplet	$\text{Rh}_4(\eta^5\text{-C}_5\text{H}_5)_4\text{H}_4 C_s$
Rh–Rh (Å)	2.61 (×2) 2.83 (×4)	2.65 (×2) 2.81 (×2) 2.82 (×2)	2.73 2.73 2.75 (×2) 2.75 (×2)	2.75 2.74 2.74 (×2) 2.75 (×2)
Rh–H (Å)	1.87 (×4) 1.85 (×4) 1.86 (×4)	1.85 (×2) 1.87 (×2) 1.87 1.86 1.86 (×2) 1.85 (×2) 1.87 (×2)	1.86 (×2) 1.87 (×2) 1.83 1.86 1.86 (×2) 1.88 (×2) 1.84 (×2)	1.84 (×2) 1.85 (×2) 1.85 (×2) 1.84 (×2) 1.84 1.83 1.83 (×2)
Rh–C (av) (Å)	2.21	2.29	2.30	2.34
$\Delta E$ (eV)		0.	0.16	

metrical distortion away from  $T_d$  is not very strong (see Figure 1 and Table 1). With four long and two short metal–metal distances (2.83 and 2.64 Å, respectively), this structure is very close to  $D_{2d}$  symmetry and strongly reminds one of compound  $2^{2+}$  (see above). Broken-symmetry calculations have also been undertaken in order to check the possibility for a singlet diradical. Unsurprisingly, they provided results that are close to those of the closed-shell singlet, with energies that are more than 0.15 eV higher.

Interestingly, the singlet/triplet energy difference is found to be very small (0.06 eV). At the current level of calculations, this value is not considered to be very accurate. Nevertheless, this small energy difference is consistent with the moderate Jahn–Teller distortion computed for the singlet state. Intuitively, one is tempted to predict that the removal of an electron pair from a saturated 60-MVE cluster would induce the formation of a M=M double bond. However, there is no pure  $\pi$ -type frontier orbital (FO) available on the Ru(arene) fragments for completing a double bond. Indeed, both  $\pi$ -type FOs of such an  $\text{ML}_3$  unit<sup>20</sup> are already involved in the three M–M single bonds. Moreover, the  $\text{Ru}(\eta^6\text{-arene})$  fragment does not possess the ligand flexibility of a simple  $\text{ML}_3$  unit, which can distort for allowing some rehybridization of its FOs. Only  $\delta$ -type FOs from the so-called “ $t_{2g}$ ” set<sup>20</sup> can be used by the Ru atoms for multiple bonding. This is actually what happens in the singlet state, where some weak multiple bonding delocalized on both short Ru–Ru bonds of the tetrahedron exists. This weak Jahn–Teller instability of compound **1**, associated with the existence of two low-lying spin states, suggests the possibility of an easy tuning of the spin state by changing the physical conditions and/or the chemical nature of the counteranion. This is why we have carried out an investigation of the magnetic behavior of  $1^{2+}$ .

Inspection of the magnetic properties (see Figure 3) revealed that, in the solid state,  $1^{2+}$  is indeed diamagnetic in the temperature range up to 300 K, with some weak temperature-independent paramagnetism, depending on the nature of the counterion: The  $\mu_{\text{eff}}/T$  diagrams of samples of  $[\mathbf{1}]\text{Cl}_2$ ,  $[\mathbf{1}][\text{BF}_4]_2$ , and  $[\mathbf{1}][\text{PF}_6]_2$  show paramagnetic contributions of 22%, 17%, and 15%, respectively, with respect to

**Figure 3.** Temperature-dependent (2–298 K) magnetization data of  $[\mathbf{1}]\text{Cl}_2$ ,  $[\mathbf{1}][\text{BF}_4]_2$ , and  $[\mathbf{1}][\text{PF}_6]_2$  in an external field of 0.1 T.**Figure 4.** Experimental vs theoretical magnetization curves of  $[\mathbf{1}]\text{Cl}_2$  computed assuming two different values for  $\Delta = E_{\text{Triplet}} - E_{\text{Singlet}}$ .

the theoretical curves for  $S = 1/2$ . Model calculations<sup>21</sup> of the temperature-dependent magnetization curve of  $[\mathbf{1}]\text{Cl}_2$  assuming different values for  $\Delta = E_{\text{Triplet}} - E_{\text{Singlet}}$  fits only when  $\Delta$  is equal or larger than 0.2 eV (Figure 4). This lower limit is rather small but significantly larger than the value computed for the free cation  $1^{2+}$  (0.06 eV).

Because the strongly related compounds  $1^{2+}$  and  $5^{2+}$  exhibit different solid-state molecular structures (pseudo- $T_d$  and pseudo- $D_{2d}$ , respectively), we have also carried out calculations on the nonmethylated model  $[\text{Rh}_4(\eta^5\text{-C}_5\text{H}_5)_4(\mu_3\text{-H})_4]^{2+}$  ( $6^{2+}$ ) and on its neutral form (**6**). The major results are given in Table 2, together with the experimental data on

(20) Albright, T. A.; Burdett, J. K.; Whangbo, M.-H. *Orbital Interactions in Chemistry*; John Wiley and Sons: New York, 1985.

(21) Kahn, O. *Molecular Magnetism*; VCH: New York, 1993.



$5^{2+}$ .<sup>17</sup> The structural trends in the  $6^{0/2+}$  series are similar to those found for the  $1^{0/2+}$  series (compare Tables 1 and 2). The singlet/triplet energy difference is found to be larger in the case of  $6^{2+}$  (0.16 eV). Accordingly, with two short and four long Rh–Rh bonds, the optimized geometry of the singlet state resembles the X-ray structure of  $5^{2+}$ .<sup>16</sup>

### Conclusions

DFT calculations on the tetrahedral cluster  $1^{2+}$  indicate that in this electron-deficient cation there is a competition between the singlet and triplet states for being the ground state. The magnetic behavior of the salts of  $1^{2+}$  in the solid state is consistent with the existence of a singlet ground state. Assuming  $1^{2+}$  to be a singlet state in the solid, the expected distortion away from  $T_d$  is not observed, while it is clearly present in the crystal structure of the tetrafluoroborate salt of  $5^{2+}$ . We suggest that, in the case of  $1^{2+}$ , the observed near- $T_d$  structure should be considered as resulting from some disorder or from the distortion due to crystal packing forces of the DFT-predicted  $C_s$  (close to  $D_{2d}$ ) geometry of the singlet state. Indeed, the computed energy difference between the

singlet  $T_d$  and  $C_s$  structures (0.28 eV) is of the same order of magnitude as the energies resulting from packing forces in such ionic crystals.

**Acknowledgment.** We thank Prof. Karl Wieghardt and Dr. Eckhard Bill, Max-Planck-Institut für Strahlenchemie, Mülheim an der Ruhr, Germany, for magnetic measurements and valuable discussions. We are grateful to Prof. Jean-Yves Pivan, Ecole Nationale Supérieure de Chimie de Rennes, Rennes, France, for his helpful comments on magnetic properties. Financial support from the Swiss National Science Foundation and the Centre National de la Recherche Scientifique as well as a generous loan of ruthenium chloride hydrate from the Johnson Matthey Research Centre are gratefully acknowledged. Computing facilities were provided by the Centre de Ressources Informatiques (CRI) of Rennes and the Institut de Développement et de Ressources en Informatique Scientifique du Centre National de la Recherche Scientifique (IDRIS-CNRS).

IC030053S